Viscoelasticity of Children and Adolescent Brains through MR Elastography

Efe Ozkaya[a,*], Gloria Fabris[a,*], Fabiola Macruz[b,*], Zeynep M. Suar[a], Javid Abderezaei[a], Bochao Su[b], Kaveh Laksari[c], Lyndia Wu[b], David B. Camarillo[b], Kim B. Pauly[b], Max Wintermark[b], Mehmet Kurt[a,d,**]

[a]*Department of Mechanical Engineering, Stevens Institute of Technology, Hoboken, NJ, 07030, USA*
[b]*Department of Radiology, Stanford University, Stanford, CA, 94305, USA*
[c]*Department of Biomedical Engineering, The University of Arizona, Tucson, AZ, 85721, USA*
[d]*Translational and Molecular Imaging Institute, Mount Sinai Icahn School of Medicine, New York, NY, 10029, USA*

Abstract

Magnetic Resonance Elastography (MRE) is an elasticity imaging technique that allows a safe, fast, and non-invasive evaluation of the mechanical properties of biological tissues *in vivo*. Since mechanical properties reflect a tissue's composition and arrangement, MRE is a powerful tool for the investigation of the microstructural changes that take place in the brain during childhood and adolescence. The goal of this study was to evaluate the viscoelastic properties of the brain in a population of healthy children and adolescents in order to identify potential age and sex dependencies. We hypothesize that because of myelination, age dependent changes in the mechanical properties of the brain will occur during childhood and adolescence. Our sample consisted of 26 healthy individuals (13 M, 13 F) with age that ranged from 7-17 years (mean: 11.9 years). We performed multifrequency MRE at 40, 60, and 80Hz actuation frequencies to acquire the complex-valued shear modulus $G = G' + iG''$ with the fundamental MRE parameters being the storage modulus (G'), the loss modulus (G''), and the magnitude of complex shear modulus ($|G|$). We fitted a springpot model to these frequency-dependent MRE parameters in order to obtain the parameter α, which is related to tissue's microstructure, and the elasticity parameter k, which was converted to a shear modulus parameter (μ) through viscosity (η). We observed no statistically significant variation in the parameter μ, but a significant increase of the microstructural parameter α of the white matter with increasing age (p <0.05). Therefore, our MRE results suggest that subtle microstructural changes such as neural tissue's enhanced alignment and geometrical reorganization during childhood and adolescence could result in significant biomechanical changes. In line with previously reported MRE data for adults, we also report significantly higher shear modulus (μ) for female brains when compared to males (p <0.05). The data presented here can serve as a clinical baseline in the analysis of the pediatric and adolescent brain's viscoelasticity over this age span, as well as extending our understanding of the biomechanics of brain development.

Keywords: Magnetic Resonance Elastography (MRE), Brain Biomechanics, Brain Development, Pediatric Brain, Brain Viscoelasticity

Introduction

The process of normal brain development unfolds according to patterns of age- and sex-related variations in the pediatric population: decades of MRI data have provided us with a richness of information on the evolution of important developmental parameters such as gray and white matter volume [1], myelination [2] and CSF content [3]. In children and adolescents, behavioral and neural changes are rapid that they parallel early postnatal development [4, 5, 6, 7], hinting at the complex, dynamical nature of this organ.

Yet, the way these and successive developmental events correlate to variations in the mechanical properties of the brain is still not completely elucidated. The mechanics of tissue has long been known to be an important hallmark of

*These authors contributed equally
**Corresponding author. Department of Mechanical Engineering, Stevens Institute of Technology, Hoboken, NJ, 07030, USA
Phone: (201) 216 - 5560.
Email address: mkurt@stevens.edu (Mehmet Kurt)

its physiological state, given that it reflects the underlying tissue microstructure [8, 9]. Therefore, in order to obtain a baseline for the mechanical and viscoelastic properties of the healthy pediatric brain, thoroughly characterizing brain stiffness at different pediatric ages is pivotal. However, such data are extremely scarce in literature, with limited age range and numbers of subjects analyzed so far [10, 11].

The most established way to probe the stiffness of a tissue is through *elastographic techniques*: these rely on the propagation of a mechanical stimulus inside the tissue and on the detection of the resulting displacement by different diagnostic imaging modalities such as ultrasound [12], computed tomography (CT) [13], or MRI [14].

In particular, magnetic resonance elastography (MRE) [15] has been gaining attention as a non-invasive means for the *in-vivo* mechanical measurement of soft tissues thanks to its capability to assess even organs as inaccessible as the brain [16, 17]. Compared to ultrasound elastography [12, 18], MRE displays higher sensitivity, does not require an acoustic window, and generates images with a higher spatial resolution [19, 20]. Clinically, MRE has been originally used to measure liver fibrosis and cirrhosis [21, 22], to characterize hepatic tumors [23], and as an alternative to liver biopsy [24], but its diagnostic use quickly spread to other types of tissue as well.

Recently, MRE has been broadly used to measure the viscoelasticity of the human brain [16, 17, 25, 26, 27]. It has quickly become a valuable tool for the indirect recognition of the changes that occur in the brain with development [10, 28], aging [29], and during the onset of many neurological conditions such as hydrocephalus [30], Alzheimer's disease [31, 32], multiple sclerosis [33, 34], or neuroinflammation [35]. A number of studies have reported brain viscoelasticity data in adults [19, 36, 37, 38, 39], adolescents [11] and animals [40, 41], but almost no published work has studied children and adolescent brains through MRE over a broad age range, with the notable exception of Yeung *et al.* [10]. In this population, MRE data acquisition is especially challenging, because it is a motion-sensitive technique in which any unwanted subject motion can cause phase errors [42, 43]. Additionally, when using this technique, cross-study comparisons can be challenging [19]: biological materials in fact display mechanical responses that are frequency-dependent, hence giving rise to a large range of values for the reported viscoelastic parameters when the actuation frequencies are not held constant. One approach to overcome this limitation is to perform multi-frequency MRE experiments and then extract frequency-independent material parameters by fitting appropriate linear viscoelastic models to the data sets [44].

In this study, we hypothesized that we would observe a stiffening behavior in the brain over the course of childhood and adolescence due to ongoing myelination and axonal pruning. We performed multifrequency MR elastography on a population of healthy children and adolescents, aged between 7 and 17. We analyzed the viscoelasticity of gray and white matter to study how this changes during the normal process of brain development. The results presented are intended to serve as a baseline for future applications of brain MRE in the pediatric population, thereby enabling viscoelasticity-based metrics to assess the pathophysiological state of brain tissue.

Material and Methods

Study population

Our study was approved by the institutional review board (IRB) of the Stanford Department of Radiology and the subjects were imaged after obtaining written informed consent from their parents and assent from study participants. Our study population consisted of 26 healthy volunteers (13 males and 13 females) of age ranging from 7-17 years (mean age of 11.9 years old) without any known neurological or psychiatric disorders. Age was considered as years completed, *e.g.* a child of 8 years and 11 months would be categorized as being 8 years old.

Image data acquisition

Conventional MRI scans were acquired by a 3.0-tesla MRI Scanner (GE, Healthcare, Waukesha, WI) at the Stanford Lucas Center for Imaging. The scanning parameters for T1-w images were set as follows: TR/TE: 9.3/3.7 ms, FOV: 240 mm, flip angle: 13 °, and acquisition matrix: 256×256 (see Figure 1b). A total of 160 slices were acquired with a slice thickness of 1.00 mm, each having a slice thickness of 1.00 mm in between. MRE images were collected on the same 3.0-tesla MRI scanner using a modified single-shot spin-echo EPI pulse sequence (MRE sequence) provided by Mayo Clinic [16, 31], in which a motion encoding gradient (MEG) was applied symmetrically around a refocusing 180-degree RF pulse [26]. A pillow like passive drum (provided by Mayo Clinic) was driven pneumatically with Resoundant system (Rochester, MN, US) under three different actuation frequencies to generate shear waves of

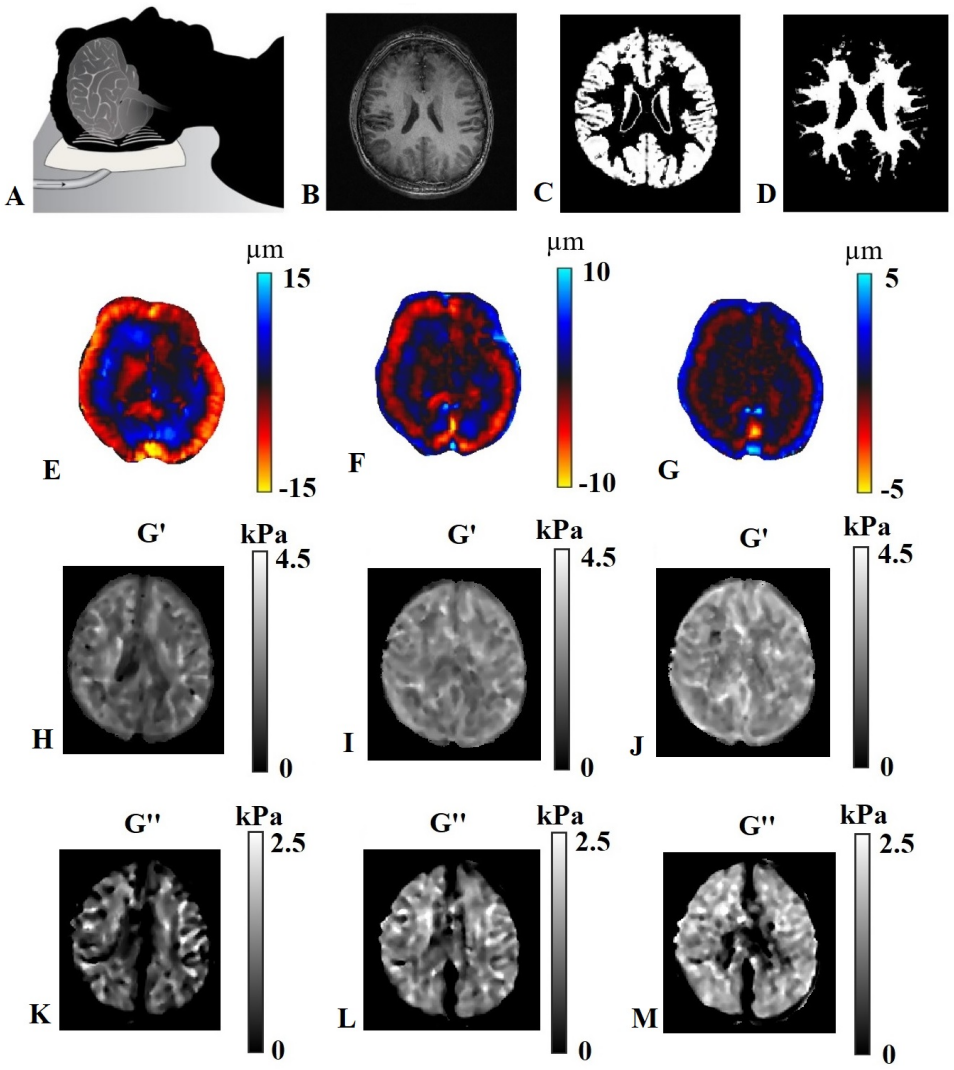

Figure 1: A) Sketch of the MRE actuation setup: A vibrating pillow below the subject's head causes shear wave propagation in the brain. B) T1-w anatomical image of a brain (subject age: 13 yrs). C) Gray matter mask. D) White matter mask. Wave propagation image for E) 40Hz, F) 60Hz, and G) 80Hz. Storage modulus ($G^{'}$) for H) 40Hz, I) 60Hz, and J) 80Hz. Loss modulus ($G^{''}$) for K) 40Hz, L) 60Hz, and M) 80Hz.

40, 60, and 80 Hz [44]. A total of 48 transverse slice with a slice thickness of 3.0 mm were acquired. For each imaging slice, through the MRE sequence 8 phase offsets of the propagating wave field were captured automatically. A head coil tuned to 128 MHz for proton resonance was used for all measurements. Each MRE image slice was acquired with the following scan parameters: TR/TE: 2000/74.5 ms for 40 Hz, 2000/62 ms for 60 Hz, and 2100/51.6 ms for 80 Hz actuation, respectively. FOV: 240 mm, and acquisition matrix: 128×128. Wave images were obtained in three orthogonal directions: frequency encoding (FE), phase encoding (PE), and slice-select (SS). To obtain the magnitude of the complex-valued shear modulus map (also known as the elastogram), wave images were processed through a 3D inversion scheme called Algebraic Inversion of the Differential Equation (AIDE) [45]. During this inversion procedure, a smoothing kernel was applied to the curl-filtered wave images. Then, the Laplacian of these wave images were calculated. Afterwards, complex-valued shear modulus maps were acquired and 3D median filter was applied as a final step. Also, the AIDE inversion accuracy was checked during the two studies published by the authors [39, 44]. Total acquisition time for all the sequences was approximately 1 hour.

Image data processing

The image post-processing steps were performed by using the SPM12 software (Welcome Trust Centre for Neuroimaging, London, UK). First, MR elastograms, storage and loss maps were registered to the same space of the T1-w images by using the coregistration option. Then, interpolation between slices was performed via a 5th degree b-spline. This step was followed by automatic segmentation of the T1-w images to obtain binary masks of white matter, gray matter and CSF regions and, by combining those, of the whole brain. Finally, the binary masks were utilized to acquire regional averaged magnitude of the complex-valued shear modulus, storage modulus and loss modulus values acquired at 40, 60, and 80 Hz actuation.

Frequency-independent parameter extraction

Currently, there are a few viscoelastic models being used to analytically represent the soft tissue response under certain loading conditions. These are Kelvin-Voigt, Maxwell, Standard Linear Solid (SLS), springpot, Burgers Model, Generalized Maxwell Model, and Fractional Voigt Model [46]. Various viscoelastic models can be fit to multifrequency MRE data in order to extract frequency-independent viscoelasticity parameters [37, 47]. Among these, we used the generic springpot and Zener models and in Matlab their analytical formulas are coded by the authors [44]. Since as highlighted in a number of studies, the springpot and Zener model (a.k.a. standard linear solid, or SLS) provide the most accurate representation of *in vivo* brain viscoelasticity data [37, 44, 19]. Furthermore, in the previously published work of the authors [44], four viscoelastic models were investigated. Springpot and Zener showed better fits than the Kelvin-Voigt and Maxwell models. Here, we initially analyzed both the springpot and Zener by fitting the corresponding viscoelastic formulations to the complex-valued shear moduli data sets $G(\omega)$ for whole brain (WB), white matter (WM), and gray matter (GM) regions. For the springpot model, this meant extracting the frequency-independent rheological parameters k and α via the fit function:

$$G = k(i\omega)^{\alpha} \tag{1}$$

where $G = G' + iG''$ is the complex-valued shear modulus. The exponent α is a parameter that has been linked to the geometrical alignment of structural building blocks in a material [37] and k is an elasticity parameter related to the shear modulus via

$$\mu = (k\eta^{-\alpha})^{\frac{1}{1-\alpha}} \tag{2}$$

where η is the viscosity. For the calculation of μ, the subject-specific viscosity η obtained from SLS model fitting was used. In the above equations ω and i denote the angular actuation frequency and the imaginary unit, respectively.

For the SLS model, the rheological parameters μ_1, μ_2 and η were calculated by fitting the expression:

$$G = (\mu_1\mu_2 + i\omega\eta(\mu_1 + \mu_2)) \,/\, (\mu_2 + i\omega\eta)) \tag{3}$$

where μ_1 the component of instantaneous elastic modulus, μ_2 the steady-state elastic modulus and η the viscosity. As the main parameters of interest an emphasis was given on the age-dependent changes of the frequency-independent rheological parameters α and k which were extracted from the springpot model fitting. Further attention was given to the shear modulus (μ) calculated by Eq. 2 since shear waves were captured through MRE imaging. In

all cases, the stiffness values presented were calculated as the magnitude of the complex-valued shear modulus via $|G| = \sqrt{(G')^2 + (G'')^2}$. All fitting procedures were performed by minimizing the fit function variance in the least-square sense via the *fmincon* function in MATLAB (v2019.b). However, to identify one preferred model to focus on, we additionally performed a Bayesian information criterion (BIC) analysis [48, 49]. During viscoelastic material model fitting, the model with the smallest BIC is chosen. The BIC criterion enables for model selection by imposing a penalty depending on the number of parameter constants that exists for each model via the computation of the quantity:

$$BIC_\omega = n\left(ln\left(\hat{\sigma}_e^2\right)\right) + d\ ln\,(n) \tag{4}$$

where $\hat{\sigma}_e^2$ is the error variance, defined as

$$\hat{\sigma}_e^2 = \frac{1}{n}\sum_{i=1}^{n}(G - G_{i,\omega})^2 \tag{5}$$

In other words, BIC attempts to reduce the risk of over fitting by introducing the penalization term $dln(n)$, which grows if the number of parameters used in a model increase [48]. In Eqs.(4) and (5), n=3 is the total number of actuation frequencies used for the data acquisition and d is the number of parameter constants that exists for each linear viscoelastic material model (*i.e.*, d=2 for the springpot model and d=3 for the SLS model). The model with the lowest BIC score would be chosen as the preferred one.

Statistical analysis

Linear regressions were performed both on frequency-dependent (G', G'', $|G|$) and frequency-independent (k, α) parameters using age and sex as covariates. Given that the interaction term resulted non-significant in all cases, we limited our analysis to a purely linear regression model without interaction terms. The level of significance was set at $p \leq 0.05$. To analyze possible sex-specific statistically significant differences in the distributions of stiffness, storage and loss modulus of the whole brain, gray matter and white matter, the two-sample t-test (MATLAB function *ttest2*) was used.

Results

Viscoelastic model selection

Global mean values for loss modulus(G''), storage modulus(G'), and stiffness($|G|$) were calculated for whole brain, gray matter, and white matter by using the binary masks generated through the SPM12 segmentation. In line with expectations, we observed generalized tissue stiffening with increasing actuation frequency. After fitting both the springpot and SLS model to the multifrequency shear and loss modulus data acquired for each subject, we performed a BIC analysis (see eq. 4) for model selection as detailed in the Materials and Methods section. The springpot performed better than the SLS model for all combinations of frequency and brain region analyzed for both loss and storage modulus (see Figures 3a and 3b, respectively). Values of the springpot BIC score were up to 10.3% lower than those of the SLS BIC, which is why in the following we limit our report to the presentation of the springpot analysis. For the interested reader, the SLS data are reported in the Supplementary Information (suppl. Table 1).

Viscoelastic properties of the human brain over the course of adolescence

When considering the evolution of the loss and storage moduli of whole brain, white matter and gray matter, no statistically significant variations with age were observed upon linear regression of the data sets at individual frequencies. The mean population values (with standard deviations) and linear regression R^2 and p-values are presented in Table 1. The overall viscoelastic parameter k evaluated from the Springpot model fit of the multifrequency data, however, showed a significant decrease with age (see Figure 4c, p-value=0.002). Once transformed via equation 2, though, the shear modulus μ appeared to not change over time (see Figure 4a). Note that, to this end, we used a group-averaged estimate for the overall brain viscosity η = 4.01 Pa.s obtained as a fit parameter of the SLS material model. Interestingly, however, the structural parameter α significantly increased over the analyzed age range (see Figure 4b), with an estimated growth of 0.002/year (p-value=0.023).

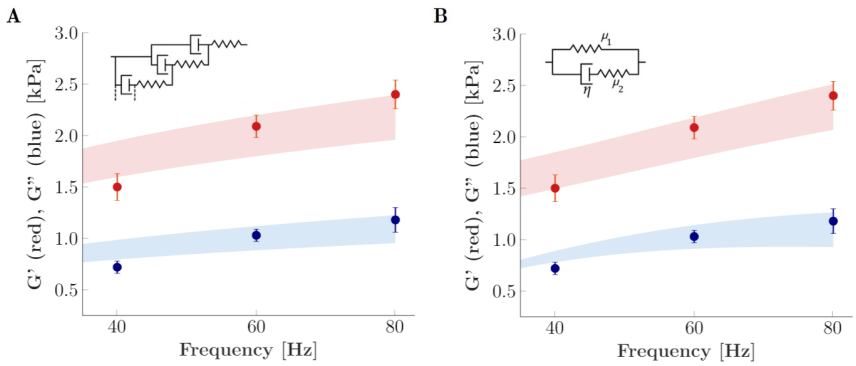

Figure 2: Viscoelastic material model fitting. Average storage (red) and loss (blue) moduli of whole brain at different actuation frequencies for the whole subject cohort with A) springpot and B) SLS model fits (shaded areas).

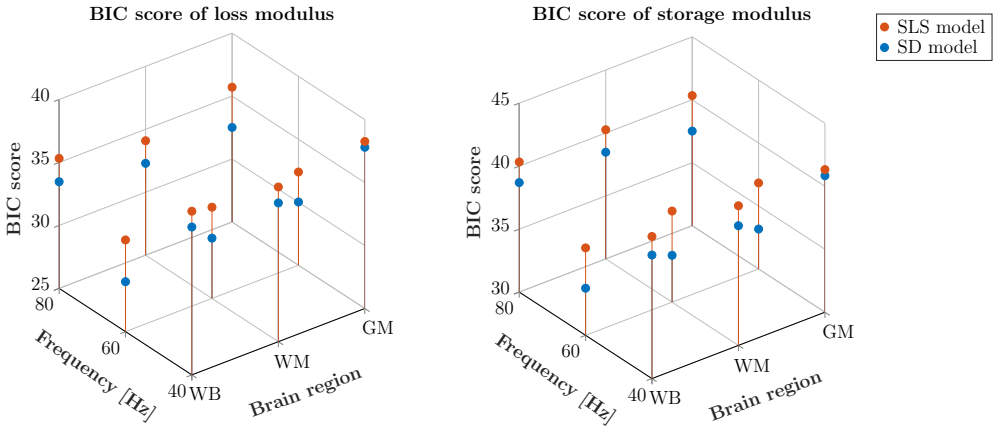

Figure 3: BIC scores as a function of actuation frequency and brain region analyzed for the SLS (Zener) model having three independent parameters while springpot (or springdashpot, SD) model having two independent parameters. The markers represent the BIC score for storage and loss moduli. The lower the BIC score, the better the model fit is. A) BIC score of the loss modulus fits. B) BIC score of the storage modulus fits. *WB*: Whole brain, *WM*: White matter, *GM*: Gray Matter.

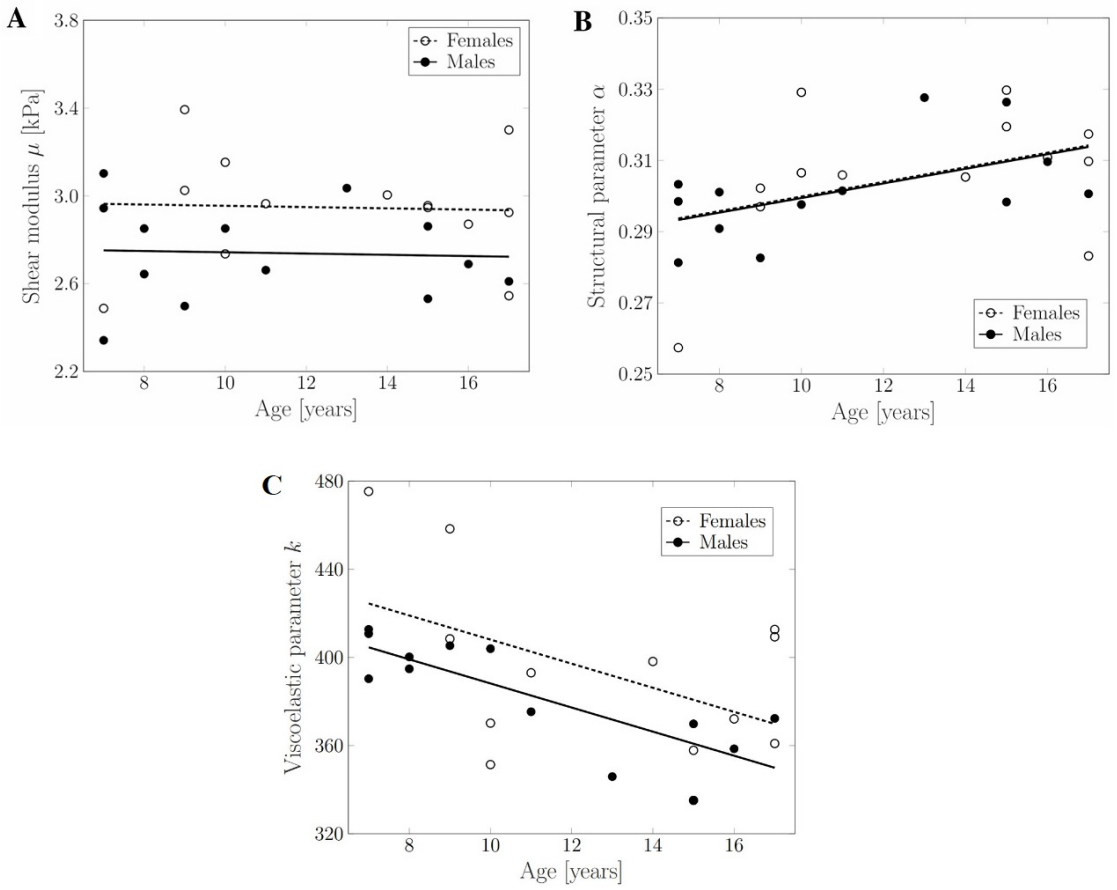

Figure 4: Age dependence of the fitted springpot model parameters for white matter. A) Shear modulus(μ) derived from Eq. 2 by using SLS model parameter viscosity(η) with the springpot model parameters k and α. B) Springpot model parameter α, which is related to the microstructural alignment, derived from Eq. 1 by fitting the fundamental MRE parameters to the springpot model. C) Age dependence of the white matter springpot model-derived parameter k for the white matter of male and female subjects. Slope: -5.46 Pa·s$^{\alpha}$/year, p-value=0.002. Fits: linear regression models using age and sex as covariates and no interaction term. Units: k=[Pa·s$^{\alpha}$]; α= dimensionless.

Table 1: Mean values of the MRE-extracted viscoelastic parameters at different actuation frequencies for all subjects, female and male cohorts, respectively. $|G|$: Magnitude of the complex-valued shear modulus, $G^{'}$: Storage Modulus, $G^{''}$: Loss Modulus. Standard deviations are in brackets. Units: [kPa]. The R^2 and p-values refer to a linear regression model using age and sex as covariates. *, ** indicate significance levels.

	Parameter [kPa]	All Subjects	Females	Males	R^2	p-value [age]	p-value [sex]
Whole Brain	$G^{''}$ (40 Hz)	0.72 (0.06)	0.73 (0.07)	0.70 (0.06)	0.10	0.29	0.16
	$G^{'}$ (40 Hz)	1.50 (0.13)	1.53 (0.14)	1.47 (0.13)	0.14	0.16	0.12
	$\|G\|$ (40 Hz)	1.69 (0.14)	1.73 (0.15)	1.66 (0.14)	0.15	0.14	0.11
	$G^{''}$ (60 Hz)	1.03 (0.06)	1.05 (0.06)	1.00 (0.06)	0.17	0.41	0.04*
	$G^{'}$ (60 Hz)	2.09 (0.11)	2.14 (0.09)	2.04 (0.11)	0.25	0.39	0.01**
	$\|G\|$ (60 Hz)	2.37 (0.13)	2.43 (0.10)	2.31 (0.12)	0.26	0.24	0.01**
	$G^{''}$ (80 Hz)	1.18 (0.12)	1.22 (0.11)	1.15 (0.12)	0.13	0.33	0.23
	$G^{'}$ (80 Hz)	2.40 (0.14)	2.45 (0.13)	2.36 (0.14)	0.11	0.90	0.12
	$\|G\|$ (80 Hz)	2.75 (0.17)	2.80 (0.15)	2.69 (0.16)	0.13	0.98	0.09
White Matter	$G^{''}$ (40 Hz)	0.80 (0.08)	0.83 (0.09)	0.78 (0.07)	0.09	0.78	0.19
	$G^{'}$ (40 Hz)	1.60 (0.12)	1.63 (0.13)	1.56 (0.1)	0.12	0.37	0.09
	$\|G\|$ (40 Hz)	1.83 (0.14)	1.87 (0.15)	1.79 (0.12)	0.11	0.50	0.11
	$G^{''}$ (60 Hz)	1.11 (0.08)	1.14 (0.09)	1.07 (0.06)	0.18	0.39	0.08
	$G^{'}$ (60 Hz)	2.14 (0.10)	2.19 (0.10)	2.09 (0.08)	0.32	0.13	0.01**
	$\|G\|$ (60 Hz)	2.45 (0.12)	2.51 (0.12)	2.39 (0.09)	0.27	0.39	0.01**
	$G^{''}$ (80 Hz)	1.19 (0.16)	1.23 (0.16)	1.15 (0.15)	0.10	0.34	0.34
	$G^{'}$ (80 Hz)	2.45 (0.16)	2.50 (0.17)	2.40 (0.13)	0.14	0.38	0.07
	$\|G\|$ (80 Hz)	2.76 (0.20)	2.83 (0.22)	2.70 (0.17)	0.11	0.79	0.11
Gray Matter	$G^{''}$ (40 Hz)	0.68 (0.06)	0.70 (0.07)	0.67 (0.05)	0.12	0.18	0.17
	$G^{'}$ (40 Hz)	1.47 (0.14)	1.50 (0.15)	1.44 (0.13)	0.13	0.17	0.15
	$\|G\|$ (40 Hz)	1.65 (0.15)	1.69 (0.16)	1.62 (0.14)	0.14	0.14	0.14
	$G^{''}$ (60 Hz)	1.00 (0.06)	1.02 (0.06)	0.98 (0.06)	0.20	0.20	0.03*
	$G^{'}$ (60 Hz)	2.07 (0.12)	2.13 (0.10)	2.02 (0.13)	0.21	0.56	0.02*
	$\|G\|$ (60 Hz)	2.35 (0.13)	2.40 (0.11)	2.29 (0.13)	0.23	0.28	0.02*
	$G^{''}$ (80 Hz)	1.18 (0.10)	1.21 (0.10)	1.15 (0.11)	0.14	0.33	0.18
	$G^{'}$ (80 Hz)	2.39 (0.15)	2.43 (0.14)	2.35 (0.15)	0.09	0.88	0.17
	$\|G\|$ (80 Hz)	2.74 (0.16)	2.80 (0.14)	2.68 (0.16)	0.12	0.89	0.10

Sex-dependent variances in the pediatric brain viscoelasticity

Analysis of the frequency-dependent viscoelastic parameters of the male and female subgroups indicated significant sex-specific differences in the complex-valued shear modulus, storage and loss modulus of whole brain, gray matter and white matter when probed at 60 Hz (see suppl. Figure 1). Mean values for the female cohort at 60 Hz increased 4.9% for the whole brain complex-valued shear modulus magnitude (p=0.015), and 4.5% and 5% for the whole brain loss and storage modulus, respectively (p=0.044, p=0.012). When analyzing the frequency-independent parameters (*i.e.*, k and α from the springpot model), this difference was no longer apparent, although a trend of stiffening for female brains remained (see Table 2).

Discussion

Despite their critical importance to understand the normal and pathological brain development, data on the mechanical properties of the pediatric brain tissue have historically been extremely scarce. Most published data are either derived from cadaver and animal studies [50, 51] or from computer simulations mimicking the response of children's

Table 2: Mean values of the springpot viscoelastic parameters k, μ and α for all subjects, and only female and male cohorts, respectively. Standard deviations are in brackets. Units: k=[Pa·s$^\alpha$]; μ=[kPa]; α=dimensionless. The R^2 and p-values refer to a linear regression model using age and sex as covariates. WB: Whole brain. WM: White matter. GM: Gray matter.

	Viscoelastic parameter	All Subjects	Females	Males	R^2	p-value [age]	p-value [sex]
WB	κ	380 (30)	387 (36)	373 (21)	0.19	0.06	0.09
	μ	2.70 (0.22)	2.78 (0.20)	2.60 (0.23)	0.16	0.63	0.04*
	α	0.30 (0.01)	0.30 (0.01)	0.30 (0.01)	0.11	0.11	0.98
WM	κ	388 (34)	392 (41)	383 (25)	0.36	0.002**	0.09
	μ	2.84 (0.25)	2.95 (0.26)	2.74 (0.22)	0.17	0.83	0.04*
	α	0.30 (0.02)	0.31 (0.02)	0.30 (0.01)	0.22	0.02*	0.95
GM	κ	380 (33)	387 (38)	372 (27)	0.11	0.24	0.17
	μ	2.64 (0.22)	2.73 (0.20)	2.56 (0.23)	0.15	0.65	0.05*
	α	0.30 (0.01)	0.30 (0.01)	0.30 (0.01)	0.06	0.26	0.99

brain to various loading conditions [52]. Recent technical advances in neuroimaging have led to the development of MRE, enabling us to finally assess the mechanical properties of the developing brain *in-vivo* and non-invasively [19]. Specifically, MRE can provide additional, indirect information about a tissue's architecture and cellular matrix, given that the viscoelasticity of a biological material reflects its micro-structural composition [53]. Even though we did not observe any statistically significant changes in shear modulus (μ) related to ageing as we hypothesized, we have observed significantly higher shear moduli (μ) in females when compared to males during childhood and adolescence. In addition, for white matter, where the myelination development occurs the most during early childhood, we observed statistically significant changes in α with aging, which is mainly due to the relation of this parameter to tissue's microstructure.

In this study, we exploit MRE to present a quantification of the mechanical properties of the pediatric and adolescent brain tissue derived from multi-frequency data. For all subjects, we observed a systematic increase in complex-valued shear modulus, storage, and loss moduli with increasing actuation frequencies, in line with expectations for a viscoelastic material. Performing linear regressions considering age and sex as covariates, we did not observe significant trends of variation with age in the mechanical properties of the brain at each single frequency. This is in line with previous work from McIlvain *et al.* [11], who characterized children's brain viscoelasticity via single-frequency MRE and reported no significant cerebrum stiffness variations between adolescents (aged 12-14 years) and young adults (aged 18-33 years). Similar observations were reported by Yeung *et al.* [10] for a cohort of children and teenagers aged between 7-18 years. There, the authors observe no relationship between the complex-valued shear modulus (G) and age or other growth metrics, concluding that the existing differences must be small in magnitude and not uniform throughout the brain [10]. These studies, however, did not analyze the frequency-independent response of the pediatric brain, which is fundamental for capturing its broadband response and understanding its dynamics during impact scenarios [54, 55, 56].

Here, we fit the frequency-dependent storage and loss modulus data to specific viscoelastic models able to analyze the overall response of the pediatric brain to actuation. In particular, we focused our analysis on the springpot model, given that it outperformed the SLS model when subject to a BIC score calculation and that it was already reported to better describe brain viscoelasticity data than other spring/dashpot combinations [37, 44]. We identified a significant decrease of the viscoelastic parameter k, which translated to a roughly constant shear modulus μ over time when transforming the quantity according to the relation $\mu = (k\eta^{-\alpha})^{\frac{1}{1-\alpha}}$ as described in [57, 37]. With population averages of $\mu = 2.6 \pm 0.2$ kPa for males and $\mu = 2.8 \pm 0.2$ kPa for females, our data are in line with those presented by Sack *et al.* [37]. In their study, a cohort of subjects aged 18 to 88 was found to undergo progressive tissue softening at the rate of -15 Pa/year. A rough extrapolation of their linear regression would predict values in the order of 2.4 kPa for males and 2.7 kPa for females around age 10, similar to the results reported here. Interestingly, we also observed a significant increase of the model exponent α with age, a result that confirms the possibility of assessing

microstructural variations of tissue *in vivo* via MR elastography [58]. The parameter α is a quantity that describes the fractal dimension of a cross-linked network of identical elements [57], with applications to rheology and polymer viscoelasticity [59]. On the other hand, another interesting parameter that can be investigated during brain maturation is fluidity, defined as phase angle. In recent work, Guo et al. analyzed the age-dependent mechanical properties of mice brain via multifrequency MRE, identifying an age-dependent increase in solid-rigid material composition and showing that after 4 weeks of maturation, a fluidity reduction is observed in the hippocampus and the corpus callosum of mice brains [60]. A retrospective analysis of the power-law behavior of different types of tissues under different pathophysiological conditions has highlighted that specific patterns of tissue degradation (*i.e.* microstructural alterations) generally lead to a decrease in both the shear modulus μ and the structural parameter α [57, 61]. In the brain, specifically, pathological conditions such as chronic multiple sclerosis (which results in diffuse myelin degradation) and the compression and dilation of the viscoelastic lattice caused by normal pressure hydrocephalus [62] are reflected in a marked decrease in α when compared to healthy brains [34]. It seems that variations in α when μ remains constant (as we report) might be associated with some sorts of re-arrangements of axonal fibers. This would be in line with the well-known anatomical data on brain myelination and white matter reorganization during adolescence [63, 64]. DTI studies have established that fractional anisotropy, along with other white matter fiber tracts alignment metrics, steadily increases until at least 18 years of age [6], as does the the G-ratio (*i.e.*, the relative axonal diameter) [65].

The reported viscoelastic differences here in white matter development are known to be sex-dependent [66, 67]. MRE studies on the effect of sex on adult brain viscoelasticity are unanimous in reporting higher complex-valued shear modulus values for female brains when compared to male ones [37, 68]. In particular, Sack *et al.* reported female brains being on average 9% stiffer than male ones [37]; here, for the whole cerebrum, we found values about half as high (4.9%). This difference might be imputed to the above-mentioned sex-related differences in white matter restructuring that takes place at different pace during development. In particular, during adolescence males seem to experience a fast, age-related white matter volume increase rooted in a testosterone-driven increase in axonal calibre [66]; whereas females appear to undergo increased myelination [66, 69], which is known to increase tissue stiffness [70].

Additionally, different brain parts follow different developmental trajectories, hence variations in brain viscoelasticity with age are expetcted to be subtle and region-specific, as already reported by [11]. In essence, all neuroimaging evidence points to the fact that a synergy of subtle biomechanical effects must be be at play during brain development: Therefore, working with larger population cohorts or performing MRE longitudinal studies would be the most valuable approach to investigate the biomechanics of development in more depth.

Some limitations must be kept in mind when considering the results of this study: first of all, we do not present data on children younger than 7 years of age, although observing how the brain's rheological properties vary during early childhood would be of paramount importance for setting a developmental baseline of brain mechanics. Due to the difficulty of recruiting and scanning young children, we could analyze only a relatively low sample population. Furthermore because of the cohort age group, it was difficult to get parental consent and perform multiple scans on the same subject to check data acquisition reproducibility. But for the analysis protocol, in the authors'previously published manuscript, MRE was performed within a frequency range from 20Hz up to 80Hz. So analysis protocol, which is used in this current study, showed reproducibility for a wider range of actuation frequencies [44]. Additionally, the space-resolution of our MRE acquisition protocol did not enable for a reliable analysis of small subcortical regions; and the direct inversion algorithm we employed (AIDE, [45]) assumes tissue isotropy, which is obviously a simplification in the case of white matter. Future studies should attempt to resolve these issues. Taken together, the data presented help fill a gap in our understanding of pediatric brain viscoelasticity, and help characterize the most prominent age and sex-related variations that occur during development.

Conclusion

In this work, we analyzed the viscoelastic properties of the pediatric and adolescent human brain measured *in vivo* via multifrequency MRE at 40, 60, and 80 Hz actuation frequencies. In line with the few previous MRE studies on developing brains [10, 11], we report no significant changes in the complex-valued shear modulus of the whole brain over the age range analyzed (7-18 years). However, by performing viscoelastic fitting of our multifrequency

data via the sprinpot model, we observed a significant increase in the structural parameter α of white matter with age while the shear modulus μ remained constant. This might be an indication of increased geometrical alignment of the material's microstructure, in line with anatomical data that report an increase of myelination and white matter fiber tract formation well into adolescence. Additionally, we assessed sex-related variations in the mechanical properties of the developing brain finding that children and adolescent female brains are stiffer than their male counterparts, as previously observed for adult subjects. In essence, the data presented aim to serve as baseline values for the analysis of pediatric brain viscoelasticity, with numerous clinical and developmental implications.

Acknowledgements

Dr. M. Kurt was the recipient of a postdoctoral fellowship from the Stanford Child Health Research Institute (CHRI). This work was funded in part by Xenith LLC.

References

[1] R. K. Lenroot, J. N. Giedd, Brain development in children and adolescents: insights from anatomical magnetic resonance imaging, Neuroscience & biobehavioral reviews 30 (6) (2006) 718–729.

[2] T. Klingberg, C. J. Vaidya, J. D. Gabrieli, M. E. Moseley, M. Hedehus, Myelination and organization of the frontal white matter in children: a diffusion tensor mri study, Neuroreport 10 (13) (1999) 2817–2821.

[3] J. Hedner, K. Lundell, G. Breese, R. Mueller, T. Hedner, Developmental variations in csf monoamine metabolites during childhood, Neonatology 49 (4) (1986) 190–197.

[4] P. M. Thompson, E. R. Sowell, N. Gogtay, J. N. Giedd, C. N. Vidal, K. M. Hayashi, A. Leow, R. Nicolson, J. L. Rapoport, A. W. Toga, Structural mri and brain development, International review of neurobiology 67 (2005) 285–323.

[5] L. P. Spear, The psychobiology of adolescence, in: Authoritative Communities, Springer, 2008, pp. 263–280.

[6] V. J. Schmithorst, W. Yuan, White matter development during adolescence as shown by diffusion mri, Brain and cognition 72 (1) (2010) 16–25.

[7] E. Toledo, A. Lebel, L. Becerra, A. Minster, C. Linnman, N. Maleki, D. W. Dodick, D. Borsook, The young brain and concussion: imaging as a biomarker for diagnosis and prognosis, Neuroscience & Biobehavioral Reviews 36 (6) (2012) 1510–1531.

[8] T. Mammoto, D. E. Ingber, Mechanical control of tissue and organ development, Development 137 (9) (2010) 1407–1420.

[9] S. Huang, D. E. Ingber, Cell tension, matrix mechanics, and cancer development, Cancer cell 8 (3) (2005) 175–176.

[10] J. Yeung, L. Jugé, A. Hatt, L. E. Bilston, Paediatric brain tissue properties measured with magnetic resonance elastography, Biomechanics and modeling in mechanobiology (2019) 1–9.

[11] G. McIlvain, H. Schwarb, N. J. Cohen, E. H. Telzer, C. L. Johnson, Mechanical properties of the in vivo adolescent human brain, Developmental cognitive neuroscience 34 (2018) 27–33.

[12] J.-L. Gennisson, T. Deffieux, M. Fink, M. Tanter, Ultrasound elastography: principles and techniques, Diagnostic and interventional imaging 94 (5) (2013) 487–495.

[13] T. Sasaki, M. Haruta, S. Omata, Ct elastography: a pilot study via a new endoscopic tactile sensor, Open Journal of Biophysics 4 (01) (2014) 22.

[14] M. M. Doyley, K. J. Parker, Elastography: general principles and clincial applications, Ultrasound clinics 9 (1) (2014) 1.

[15] R. Muthupillai, D. Lomas, P. Rossman, J. F. Greenleaf, A. Manduca, R. Ehman, Magnetic resonance elastography by direct visualization of propagating acoustic strain waves, science 269 (5232) (1995) 1854–1857.

[16] S. A. Kruse, G. H. Rose, K. J. Glaser, A. Manduca, J. P. Felmlee, C. R. Jack Jr, R. L. Ehman, Magnetic resonance elastography of the brain, Neuroimage 39 (1) (2008) 231–237.

[17] M. A. Green, L. E. Bilston, R. Sinkus, In vivo brain viscoelastic properties measured by magnetic resonance elastography, NMR in Biomedicine: An International Journal Devoted to the Development and Application of Magnetic Resonance In vivo 21 (7) (2008) 755–764.

[18] D. Chauvet, M. Imbault, L. Capelle, C. Demene, M. Mossad, C. Karachi, A.-L. Boch, J.-L. Gennisson, M. Tanter, In vivo measurement of brain tumor elasticity using intraoperative shear wave elastography, Ultraschall in der Medizin-European Journal of Ultrasound 37 (06) (2016) 584–590.

[19] L. V. Hiscox, C. L. Johnson, E. Barnhill, M. D. McGarry, J. Huston 3rd, E. J. Van Beek, J. M. Starr, N. Roberts, Magnetic resonance elastography (mre) of the human brain: technique, findings and clinical applications, Physics in Medicine & Biology 61 (24) (2016) R401.

[20] P. J. McCracken, A. Manduca, J. Felmlee, R. L. Ehman, Mechanical transient-based magnetic resonance elastography, Magnetic Resonance in Medicine: An Official Journal of the International Society for Magnetic Resonance in Medicine 53 (3) (2005) 628–639.

[21] O. Rouviere, M. Yin, M. A. Dresner, P. J. Rossman, L. J. Burgart, J. L. Fidler, R. L. Ehman, Mr elastography of the liver: preliminary results, Radiology 240 (2) (2006) 440–448.

[22] R. Loomba, T. Wolfson, B. Ang, J. Hooker, C. Behling, M. Peterson, M. Valasek, G. Lin, D. Brenner, A. Gamst, et al., Magnetic resonance elastography predicts advanced fibrosis in patients with nonalcoholic fatty liver disease: a prospective study, Hepatology 60 (6) (2014) 1920–1928.

[23] S. K. Venkatesh, M. Yin, J. F. Glockner, N. Takahashi, P. A. Araoz, J. A. Talwalkar, R. L. Ehman, Mr elastography of liver tumors: preliminary results, American Journal of Roentgenology 190 (6) (2008) 1534–1540.

[24] H. Morisaka, U. Motosugi, S. Ichikawa, T. Nakazawa, T. Kondo, S. Funayama, M. Matsuda, T. Ichikawa, H. Onishi, Magnetic resonance elastography is as accurate as liver biopsy for liver fibrosis staging, Journal of Magnetic Resonance Imaging 47 (5) (2018) 1268–1275.
[25] J. Huston, Magnetic resonance elastography of the brain, in: Magnetic resonance elastography, Springer, 2014, pp. 89–98.
[26] M. C. Murphy, J. Huston III, C. R. Jack Jr, K. J. Glaser, M. L. Senjem, J. Chen, A. Manduca, J. P. Felmlee, R. L. Ehman, Measuring the characteristic topography of brain stiffness with magnetic resonance elastography, PloS one 8 (12) (2013) e81668.
[27] E. Clayton, J. Garbow, P. Bayly, Frequency-dependent viscoelastic parameters of mouse brain tissue estimated by mr elastography, Physics in Medicine & Biology 56 (8) (2011) 2391.
[28] C. L. Johnson, E. H. Telzer, Magnetic resonance elastography for examining developmental changes in the mechanical properties of the brain, Developmental cognitive neuroscience (2017).
[29] I. Sack, K.-J. Streitberger, D. Krefting, F. Paul, J. Braun, The influence of physiological aging and atrophy on brain viscoelastic properties in humans, PloS one 6 (9) (2011) e23451.
[30] N. Fattahi, A. Arani, A. Perry, F. Meyer, A. Manduca, K. Glaser, M. Senjem, R. L. Ehman, J. r. Huston, Mr elastography demonstrates increased brain stiffness in normal pressure hydrocephalus, American Journal of Neuroradiology 37 (3) (2016) 462–467.
[31] M. C. Murphy, J. Huston III, C. R. Jack Jr, K. J. Glaser, A. Manduca, J. P. Felmlee, R. L. Ehman, Decreased brain stiffness in alzheimer's disease determined by magnetic resonance elastography, Journal of magnetic resonance imaging 34 (3) (2011) 494–498.
[32] M. C. Murphy, D. T. Jones, C. R. Jack Jr, K. J. Glaser, M. L. Senjem, A. Manduca, J. P. Felmlee, R. E. Carter, R. L. Ehman, J. Huston III, Regional brain stiffness changes across the alzheimer's disease spectrum, NeuroImage: Clinical 10 (2016) 283–290.
[33] J. Wuerfel, F. Paul, B. Beierbach, U. Hamhaber, D. Klatt, S. Papazoglou, F. Zipp, P. Martus, J. Braun, I. Sack, Mr-elastography reveals degradation of tissue integrity in multiple sclerosis, Neuroimage 49 (3) (2010) 2520–2525.
[34] K.-J. Streitberger, I. Sack, D. Krefting, C. Pfüller, J. Braun, F. Paul, J. Wuerfel, Brain viscoelasticity alteration in chronic-progressive multiple sclerosis, PloS one 7 (1) (2012) e29888.
[35] A. Fehlner, J. R. Behrens, K.-J. Streitberger, S. Papazoglou, J. Braun, J. Bellmann-Strobl, K. Ruprecht, F. Paul, J. Würfel, I. Sack, Higher-resolution mr elastography reveals early mechanical signatures of neuroinflammation in patients with clinically isolated syndrome, Journal of Magnetic Resonance Imaging 44 (1) (2016) 51–58.
[36] I. Sack, B. Beierbach, U. Hamhaber, D. Klatt, J. Braun, Non-invasive measurement of brain viscoelasticity using magnetic resonance elastography, NMR in Biomedicine: An International Journal Devoted to the Development and Application of Magnetic Resonance In vivo 21 (3) (2008) 265–271.
[37] I. Sack, B. Beierbach, J. Wuerfel, D. Klatt, U. Hamhaber, S. Papazoglou, P. Martus, J. Braun, The impact of aging and gender on brain viscoelasticity, Neuroimage 46 (3) (2009) 652–657.
[38] C. L. Johnson, M. D. McGarry, A. A. Gharibans, J. B. Weaver, K. D. Paulsen, H. Wang, W. C. Olivero, B. P. Sutton, J. G. Georgiadis, Local mechanical properties of white matter structures in the human brain, Neuroimage 79 (2013) 145–152.
[39] H. Lv, M. Kurt, N. Zeng, E. Ozkaya, F. Marcuz, L. Wu, K. Laksari, D. B. Camarillo, K. B. Pauly, Z. Wang, et al., Mr elastography frequency–dependent and independent parameters demonstrate accelerated decrease of brain stiffness in elder subjects, European Radiology (2020) 1–10.
[40] J. D. Finan, B. S. Elkin, E. M. Pearson, I. L. Kalbian, B. Morrison, Viscoelastic properties of the rat brain in the sagittal plane: effects of anatomical structure and age, Annals of biomedical engineering 40 (1) (2012) 70–78.
[41] A. Gefen, N. Gefen, Q. Zhu, R. Raghupathi, S. S. Margulies, Age-dependent changes in material properties of the brain and braincase of the rat, Journal of neurotrauma 20 (11) (2003) 1163–1177.
[42] M. C. Murphy, J. Huston 3rd, K. Glaser, A. Manduca, J. Felmlee, et al., Phase correction for interslice discontinuities in multislice epi mr elastography, Montreal (2012) 3426.
[43] C. L. Johnson, M. D. McGarry, E. E. Van Houten, J. B. Weaver, K. D. Paulsen, B. P. Sutton, J. G. Georgiadis, Magnetic resonance elastography of the brain using multishot spiral readouts with self-navigated motion correction, Magnetic resonance in medicine 70 (2) (2013) 404–412.
[44] M. Kurt, L. Wu, K. Laksari, E. Ozkaya, Z. M. Suar, H. Lv, K. Epperson, K. Epperson, A. M. Sawyer, D. Camarillo, et al., Optimization of a multifrequency magnetic resonance elastography protocol for the human brain, Journal of Neuroimaging (2019).
[45] T. E. Oliphant, A. Manduca, R. L. Ehman, J. F. Greenleaf, Complex-valued stiffness reconstruction for magnetic resonance elastography by algebraic inversion of the differential equation, Magnetic Resonance in Medicine: An Official Journal of the International Society for Magnetic Resonance in Medicine 45 (2) (2001) 299–310.
[46] B. Zhou, X. Zhang, Comparison of five viscoelastic models for estimating viscoelastic parameters using ultrasound shear wave elastography, Journal of the mechanical behavior of biomedical materials 85 (2018) 109–116.
[47] R. Sinkus, K. Siegmann, T. Xydeas, M. Tanter, C. Claussen, M. Fink, Mr elastography of breast lesions: understanding the solid/liquid duality can improve the specificity of contrast-enhanced mr mammography, Magnetic Resonance in Medicine: An Official Journal of the International Society for Magnetic Resonance in Medicine 58 (6) (2007) 1135–1144.
[48] G. Schwarz, et al., Estimating the dimension of a model, The annals of statistics 6 (2) (1978) 461–464.
[49] H. S. Bhat, N. Kumar, On the derivation of the bayesian information criterion, School of Natural Sciences, University of California (2010).
[50] S. Chatelin, J. Vappou, S. Roth, J.-S. Raul, R. Willinger, Towards child versus adult brain mechanical properties, Journal of the mechanical behavior of biomedical materials 6 (2012) 166–173.
[51] A.-C. Duhaime, S. S. Margulies, S. R. Durham, M. M. O'Rourke, J. A. Golden, S. Marwaha, R. Raghupathi, Maturation-dependent response of the piglet brain to scaled cortical impact, Journal of neurosurgery 93 (3) (2000) 455–462.
[52] S. Cui, Y. Chen, H. Li, L. He, S. Ruan, Effects of brain mechanical properties on child head responses under linear load, Biomedical Engineering Letters 6 (2) (2016) 87–93.
[53] C. L. Johnson, E. H. Telzer, Magnetic resonance elastography for examining developmental changes in the mechanical properties of the brain, Developmental cognitive neuroscience 33 (2018) 176–181.
[54] J. Abderezaei, W. Zhao, C. L. Grijalva, G. Fabris, S. Ji, K. Laksari, M. Kurt, Nonlinear dynamical behavior of the deep white matter during head impact, Physical Review Applied 12 (1) (2019) 014058.
[55] K. Laksari, M. Kurt, H. Babaee, S. Kleiven, D. Camarillo, Mechanistic insights into human brain impact dynamics through modal analysis,

Physical review letters 120 (13) (2018) 138101.
[56] A. Mojahed, J. Abderezaei, M. Kurt, L. A. Bergman, A. F. Vakakis, A nonlinear reduced-order model of the corpus callosum under planar coronal excitation, Journal of Biomechanical Engineering 142 (9) (2020).
[57] I. Sack, K. Jöhrens, J. Würfel, J. Braun, Structure-sensitive elastography: on the viscoelastic powerlaw behavior of in vivo human tissue in health and disease, Soft Matter 9 (24) (2013) 5672–5680.
[58] J. Guo, O. Posnansky, S. Hirsch, M. Scheel, M. Taupitz, J. Braun, I. Sack, Fractal network dimension and viscoelastic powerlaw behavior: Ii. an experimental study of structure-mimicking phantoms by magnetic resonance elastography, Physics in Medicine & Biology 57 (12) (2012) 4041.
[59] O. Posnansky, J. Guo, S. Hirsch, S. Papazoglou, J. Braun, I. Sack, Fractal network dimension and viscoelastic powerlaw behavior: I. a modeling approach based on a coarse-graining procedure combined with shear oscillatory rheometry, Physics in Medicine & Biology 57 (12) (2012) 4023.
[60] J. Guo, G. Bertalan, D. Meierhofer, C. Klein, S. Schreyer, B. Steiner, S. Wang, R. V. da Silva, C. Infante-Duarte, S. Koch, et al., Brain maturation is associated with increasing tissue stiffness and decreasing tissue fluidity, Acta Biomaterialia 99 (2019) 433–442.
[61] S. Yoshida, K. Oishi, A. V. Faria, S. Mori, Diffusion tensor imaging of normal brain development, Pediatric radiology 43 (1) (2013) 15–27.
[62] F. B. Freimann, K.-J. Streitberger, D. Klatt, K. Lin, J. McLaughlin, J. Braun, C. Sprung, I. Sack, Alteration of brain viscoelasticity after shunt treatment in normal pressure hydrocephalus, Neuroradiology 54 (3) (2012) 189–196.
[63] T. Paus, A. Zijdenbos, K. Worsley, D. L. Collins, J. Blumenthal, J. N. Giedd, J. L. Rapoport, A. C. Evans, Structural maturation of neural pathways in children and adolescents: in vivo study, Science 283 (5409) (1999) 1908–1911.
[64] D. J. Miller, T. Duka, C. D. Stimpson, S. J. Schapiro, W. B. Baze, M. J. McArthur, A. J. Fobbs, A. M. Sousa, N. Šestan, D. E. Wildman, et al., Prolonged myelination in human neocortical evolution, Proceedings of the National Academy of Sciences 109 (41) (2012) 16480–16485.
[65] T. Paus, Growth of white matter in the adolescent brain: myelin or axon?, Brain and cognition 72 (1) (2010) 26–35.
[66] J. S. Perrin, G. Leonard, M. Perron, G. B. Pike, A. Pitiot, L. Richer, S. Veillette, Z. Pausova, T. Paus, Sex differences in the growth of white matter during adolescence, Neuroimage 45 (4) (2009) 1055–1066.
[67] R. K. Lenroot, N. Gogtay, D. K. Greenstein, E. M. Wells, G. L. Wallace, L. S. Clasen, J. D. Blumenthal, J. Lerch, A. P. Zijdenbos, A. C. Evans, et al., Sexual dimorphism of brain developmental trajectories during childhood and adolescence, Neuroimage 36 (4) (2007) 1065–1073.
[68] A. Arani, M. C. Murphy, K. J. Glaser, A. Manduca, D. S. Lake, S. A. Kruse, C. R. Jack Jr, R. L. Ehman, J. Huston 3rd, Measuring the effects of aging and sex on regional brain stiffness with mr elastography in healthy older adults, Neuroimage 111 (2015) 59–64.
[69] T. Paus, R. Toro, Could sex differences in white matter be explained by g ratio?, Frontiers in neuroanatomy 3 (2009) 14.
[70] J. Weickenmeier, R. de Rooij, S. Budday, P. Steinmann, T. Ovaert, E. Kuhl, Brain stiffness increases with myelin content, Acta biomaterialia 42 (2016) 265–272.